Energy-aware Approaches for Energy Harvesting Powered Wireless Sensor Nodes

Tingwen Ruan, Zheng Jun Chew, *Member, IEEE* and Meiling Zhu, *Member, IEEE*

***Abstract*— Intensive research on energy harvesting powered wireless sensor nodes (WSNs) has been driven by the needs of reducing the power consumption by the WSNs and the increasing the power generated by energy harvesters. The mismatch between the energy generated by the harvesters and the energy demanded by the WSNs is always a bottleneck as the ambient environmental energy is limited and time-varying. This paper introduces a combined energy-aware interface (EAI) with an energy-aware program to deal with the mismatch through managing the energy flow from the energy storage capacitor to the WSNs. These two energy-aware approaches were implemented in a custom developed vibration energy harvesting powered WSN. The experimental results show that, with the 3.2 mW power generated by a piezoelectric energy harvester (PEH) under an emulated aircraft wing strain loading of 600 με at 10 Hz, the combined energy-aware approaches enable the WSN to have a significantly reduced sleep current from 28.3 μA of a commercial WSN to 0.95 μA and enable the WSN operations for a long active time of about 1.15 s in every 7.79 s to sample and transmit a large number of data (388 bytes), rather than a few ten milliseconds and a few bytes, as demanded by vibration measurement. When the approach was not used, the same amount of energy harvested was not able to power the WSN to start, not mentioning to enabling the WSN operation, which highlighted the importance and the value of the energy-aware approaches in enabling energy harvesting powered WSN operation successfully.**

***Index Terms*— energy harvesting, energy-aware interface, energy-aware program, wireless sensor nodes**

I. Introduction

In the last decade there has been an increasing interest on the development of energy harvesting powered wireless sensing nodes (WSNs) for applications such as healthcare, industrial process monitoring, environment monitoring, and structural health monitoring [1, 2]. This is because the energy harvesting powered WSNs can operate for years and years without the needs of human intervention for battery replacements. However, to date, there are a few implementations in such WSNs. The main reason is that the energy generated by energy harvesters is not high enough for powering the WSNs as commercially available WSNs are power hungry. This means there is a mismatch between the energy generated by the harvesters and the energy demanded by the WSNs to perform the required tasks. Therefore, there is a need to deal with this mismatch by reducing the power consumption of WSNs and increasing the amount of power that can be harvested and/or extracted to the WSN.

To increase the power harvested and extract more power to the WSN, since the energy that can be scavenged by an energy harvester is highly dependent on the types of energy harvesters and the environmental conditions [2], a more practical approach is to place a power management module (PMM) in between the energy harvester and the WSN to manage the energy mismatch by harvesting as much power as possible from the energy harvester under various conditions. A large number of PMMs have been proposed to improve the amount of harvested energy. Typical methods were based on nonlinear techniques for extracting as high power as possible typically in piezoelectric [3, 4] and electromagnetic [5, 6] energy harvesting and resistive/impedance matching for maximum power transfer from the energy harvesters to the loads in all types of energy harvesting such as solar [7], thermoelectric [8], piezoelectric [9], and electromagnetic energy harvesting [10]. In the nonlinear techniques, switches are toggled at appropriate timing to momentarily form an *LC* oscillator circuit using the energy harvesters and external components such as inductor [3, 4] or capacitor [5, 6]. The oscillation occurred increases the voltage waveforms from the energy harvesters, and hence the power is increased. Maximum power transfer occurs when the impedances of both the energy harvesters and connected loads are matched. In the resistive/impedance matching techniques, a DC–DC converter is usually used to emulate the modulus of the impedance of an energy harvester by dynamically changes its duty cycle. It should be noted that a WSN can be seen as a dynamic load as it consumes different amount of current when it is performing different tasks [11]. Therefore, the amount of energy that can be harvested using these techniques will still be affected by the connected WSNs due to the loading effect brought by the dynamism of WSNs. Direct connection of the WSNs to the PMMs will drastically reduce the amount of power that can be harvested [12].

To reduce the power consumption of the WSNs, one of the common approaches is to choose low sleep power consumption wireless microcontrollers (MCUs). Off-the-shelf MCUs which are the core part of the WSNs have ultra-low sleep power consumption but they are characterized in the conditions that a small sized memory is attached and a few peripheral devices are connected to the MCUs. For example, the current consumptions are 0.7 μA with 1.8 V supply voltage for

This work was supported by the Engineering and Physical Sciences Research Council (EPSRC) in the UK via the projects entitled "SMARTER-Smart Multifunction Architecture & Technology for Energy-aware Wireless Sensors" EP/K017950/1 and "En-ComE-Energy Harvesting Powered Wireless Monitoring Systems Based on Integrated Smart Composite Structures and Energy-Aware Architecture" EP/K020331/1.

The authors are with Energy Harvesting Group at University of Exeter, EX4 4QF, Exeter, UK. (email: tr287@exeter.ac.uk; z.j.chew@exeter.ac.uk; m.zhu@exeter.ac.uk)

MSP430 of Texas Instruments in an ultra-low power standby mode [13] and 2.6 µA for Jennic with an active sleep timer from NXP in a sleep mode [14]. In practical applications, there are a large sized memory attached and many peripheral devices connected with the MCUs, which include crystal and resistor-capacitor oscillators, sensor interface circuits and transmission circuits. The current consumptions of these devices have not been included in the datasheets of the MCUs. This means the actual power consumptions of the WSNs during the sleep modes are usually much higher than the ones provided in the datasheets. The high sleep power consumption would cause a start-up problem for energy harvesting powered WSNs when there is a limited energy harvested since energy could not be accumulated, leading to voltage in the energy storage capacitor lower than the minimum operation voltage of the MCUs. Therefore, the MCUs are not able to become active and play their functions in controlling their sub-circuits such as wake-up timers, digital input/output (DIO) blocks, comparators, and resistor-capacitor oscillators through software programmed in the flash memory of the MCUs. The worst thing is that, although the MCUs are not able to start, the connected sub-circuits are still continually consuming energy in the energy storage capacitor, making the WSN never ever be able to start its operation.

In order to solve the start-up problem and the loading effect of a WSN on a PMM, reviewed above, a few attempts have been made to develop an energy-aware interface (EAI) between the PMM and the WSNs to manage the energy flow from the energy storage of capacitor to and activate the WSNs. For example, Minami et al. [15] introduced the use of a CMOS reset IC (ROHM BD4835G) to reset their solar energy harvesting powered WSN when the voltage across the supercapacitor is lower than 3.5 V. Torah et al. [14] introduced a cold start circuit which ensures that the MCU will only begin to draw power from the storage capacitor and start up when a minimum voltage of 2 V is met. Also, Torah et al. introduced the use of a MCU to determine the energy availability by monitoring voltage across a supercapacitor and adjust the measurement duty cycle based on the energy availability to keep the voltage across the supercapacitor steady at around 2.2 V. However, this method has limited the system to a low duty cycle operation and small data packet size for wireless transmission. Zhu et al. [16] and Ferrari et al. [17] reported the use of an energy-aware interface to turn on and turn off the WSN based on the pre-fixed voltages which are defined as turn-on and turn-off voltage thresholds respectively in their developed piezoelectric energy harvesting powered system. However, there is a drawback of such an EAI that the WSNs would stay active until the pre-fixed turn-off voltage threshold reached regardless of the WSN operation states. For example, if the WSNs finish the tasks early, this could cause wastage energy as the WSN is still on; if the WSN is in the period of operation, this would cause the WSNs to be unable to finish the required tasks as the turn-off voltage threshold is reached. This is not ideal for real applications to use such a pre-fixed voltage threshold hardware switching approach. In order to utilize the energy stored in the capacitor more effectively, this paper will, on top of the EAI, introduce an energy-aware program by monitoring the voltage in the capacitor to judge if there is enough energy in the capacitor for the WSNs to carry out the next operation and ensure all the measured data is transmitted before the energy becomes too low for operation of the WSNs. The energy-aware program is especially suitable for structural health monitoring of vibration [18] as the WSNs are required to turn on as long as possible for as many sampling data as possible without the limitation of constrained duty-cycle, which will be studied in this paper.

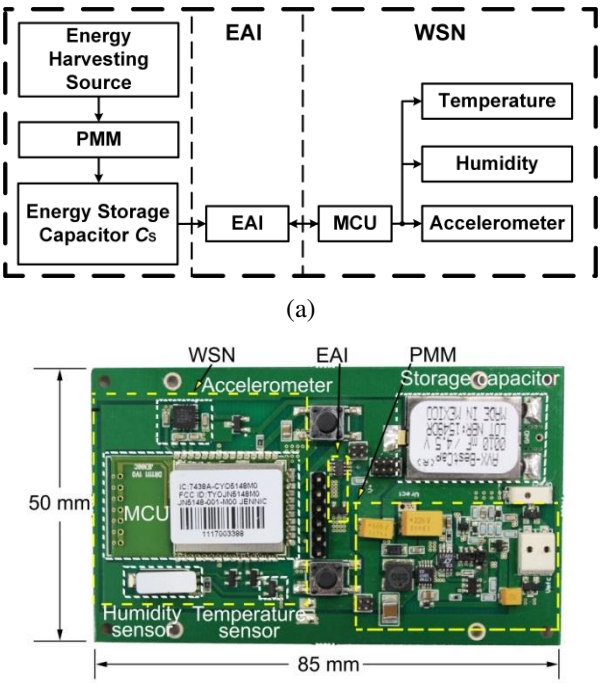

Fig. 1. (a) Block diagram of the custom developed energy harvesting powered WSN with the EAI and (b) the image of prototyped PCB of the developed energy harvesting powered WSN.

This paper therefore introduces a combined energy-aware interface (EAI) with an energy-aware program to manage the energy flow from the energy storage capacitor to WSNs and deal with the energy mismatch for enabling the operation of WSN. These hardware and software energy-aware approaches are implemented in a custom developed vibration energy harvesting powered WSN. The energy-aware approaches are experimentally studied to understand the advantage of the introduced energy-aware approaches in overcoming the high sleep power consumption during sleep time of the WSN that causes the start-up problem and in enabling the energy harvesting powered WSN operation for maximum data sampling and transmitting with a limited energy generated by the harvester.

II. System Description

Fig. 1 (a) illustrates the block diagram of the custom developed energy harvesting powered WSN with the EAI. It is composed of three main blocks: (i) an energy harvesting source with a PMM and an energy storage capacitor C_S, (ii) an EAI and (iii) an energy-aware WSN. An image of the implemented printed circuit board (PCB) with the EAI and the WSN is shown in the Fig. 1 (b). A piezoelectric strain energy harvester using a macro-fiber composite (MFC) is used to scavenge

ambient vibrational energy to charge up the capacitor through the PMM, where the accumulated energy stored in the capacitor C_S is used to power the WSN. It should be noted that the developed energy-aware WSN is suitable for all types of vibration harvesters connected with different PMMs and therefore the harvester and the PMM will not be discussed in this paper. The EAI, which serves as the interface between the PMM and the WSN, plays an important role in operating the WSN, and therefore will be discussed in detail below.

A. EAI Circuit and its Operation

Fig. 2 (a) shows the schematic of the EAI circuit which comprises a voltage supervisor (LTC2935-1, Linear Technology, United States) to monitor the voltage across the capacitor V_{cs} and an N-MOSFET to switch on or off the WSN.

Fig. 2 (b) shows the illustration of the voltage V_{CS} changes under the control of EAI. The V_{on} is the pre-fixed voltage threshold set by the voltage supervisor to turn on the WSN to perform its measurement tasks. The V_{end} is the calculated voltage by the MCU, indicating that the capacitor will not have enough energy for the WSN to perform the next measurement tasks and the WSN should end its measurement operation. The V_{off} is the voltage that the WSN will be turned off after the MCU transmitted all the sampled and stored data. The V_{min} is the minimum operating voltage of the WSN and below V_{min}, the WSN is no longer able to operate properly. Therefore, V_{end} is higher than V_{off}, and V_{off} is higher than V_{min}, giving an extra margin to the energy availability for performing the tasks and ensuring that the WSN can successfully sample and transmit all the data before V_{CS} drops below $V_{min.}$. The relationships among the voltages are $V_{on} > V_{end} > V_{off} > V_{min}$, shown in Fig. 2 (b).

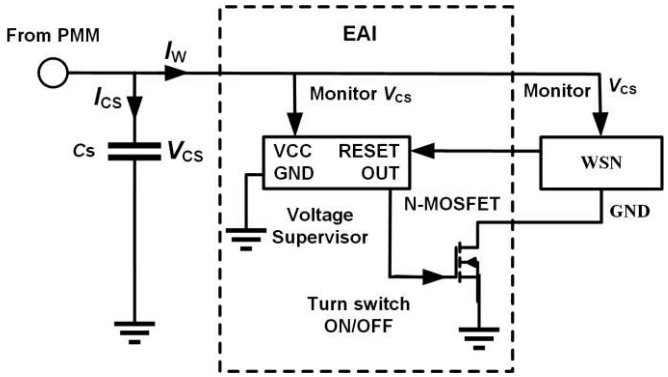

(a)

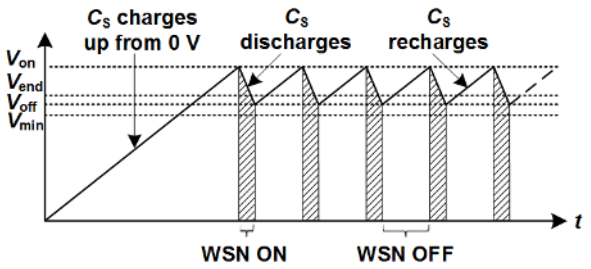

(b)

Fig. 2. (a) Schematic of the hardware EAI and (b) an illustration of the voltage V_{CS} changes across the capacitor under the control of EAI.

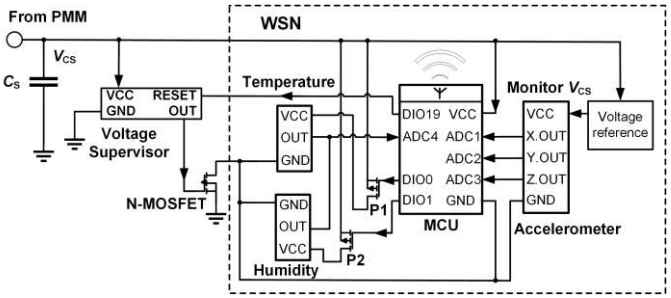

Fig. 3. Schematic of the developed WSN connected with the EAI.

It should be noted that V_{end} is not the turn-off voltage threshold of the voltage supervisor and also not pre-fixed voltages. V_{end} is determined not only by the energy stored in the capacitor C_S but also by the energy required by the WSN for the next operation, which will be studied in Subsection D.

The operation is explained as follows. The capacitor C_S is initially charged from 0 V and the output pin of the EAI keeps low when V_{CS} is lower than the voltage supervisor turn-on threshold V_{on}. Once V_{CS} exceeds the turn-on threshold V_{on}, the output pin is set to be in a high state, which places the N-MOSFET transistor in a low impedance state, connecting the system and WSN ground. The WSN and the capacitor C_S then form a closed circuit, where the current can be drawn by the WSN, and consequently the WSN is enabled to become active to carry out the programmed tasks, where I_w is the current input to the WSN and EAI, and I_{CS} is the current input to the capacitor C_S. During the active phase, the WSN monitors V_{CS} and uses the energy-aware program to judge whether there is enough energy in the capacitor C_S for the WSN to carry out the next operation, that is, V_{CS} is larger than V_{end}. If V_{CS} is lower than $V_{end,}$ the WSN finishes off its task immediately and then resets the voltage supervisor to turn off the N-MOSFET switch. As a result, the WSN is disconnected from C_S and is turned to the non-active phase so that the capacitor can be charged up again if there is input energy from the harvester. The system will remain in the non-active phase until V_{CS} reaches V_{on} again, and then the cycles repeat.

B. Wireless Sensor Node

The schematic of the developed WSN for this study is shown in Fig. 3. The WSN is built using a wireless MCU and three analogue sensors. The MCU used is Jennic JN5148 (NXP Semiconductors, Eindhoven, Netherlands) which has a 2.4 GHz IEEE 802.15.4 compliant transceiver to communicate using ZigBee protocol, 128 kB of read-only memory (ROM) and random access memory (RAM) each. The sensors used are ADXL335 3-axis accelerometer (Analog Devices, Massachusetts, USA), a MCP9700 temperature sensor (Microchip Technology, Inc., Arizona, USA), and a low voltage humidity sensor (HIH-5030, Honeywell, New Jersey, USA). All of them are chosen based on the low power consumption and small amount of linear signal processing required, since the top consideration in the design of WSN is low energy consumption. The output pin of all sensors can be directly connected to the analogue-to-digital converter (ADC) input of the MCU. However, the MCU only has 4 ADC pins,

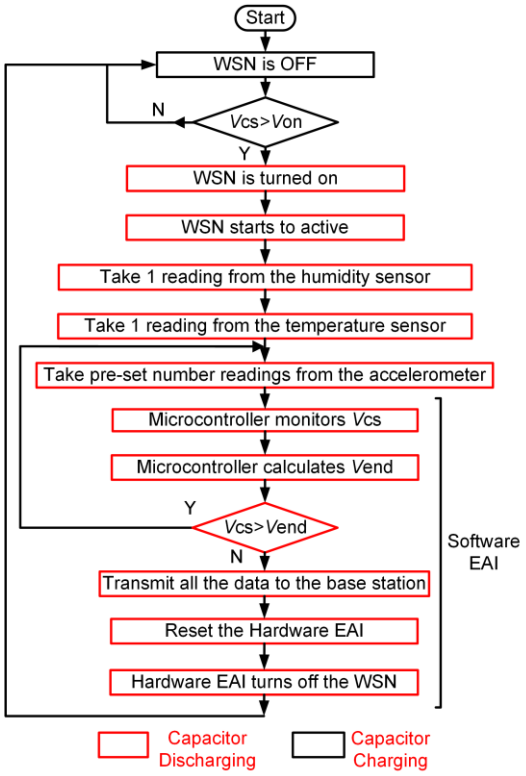

Fig. 4. Flowchart of the operation cycle of the energy-aware programmed WSN by software.

which is not enough for 5 ADC readings from the three sensors. Therefore, the temperature and humidity sensor are designed to share the ADC4 pin, which are switched on and off successively by the P-MOSFETs controlled using DIO pins of the MCU to prevent conflict between the sensors which could lead to data loss or corruption if they were both on all the time. The remaining three ADCs are individually connected to the three outputs (acceleration in x-, y- and z-axis) of the 3-axis accelerometer. In contrast, continuous data reading from the accelerometer is required because the accelerations are highly dynamic and change rapidly. Given that V_{CS} is not constant throughout the active phase for the accelerometer which requires a fixed reference voltage to determine the accelerations from the sensor readings, a voltage reference (ISL21080CIH325, Intersil, California, USA) is used to provide a fixed reference voltage of 2.5 V to the accelerometer during the active time of the WSN. Humidity and temperature do not require continuous measurement since these quantities do not change as rapidly as the acceleration does.

C. *Energy-aware programmed WSN*

The operation flowchart of the energy-aware programmed WSN is shown in Fig. 4. The operation begins with the WSN in non-active phase until there is enough energy in the capacitor C_S to turn on the MCU. Once there is sufficient energy in the capacitor C_S, the voltage supervisor turns on the N-MOSFET, which in turn switches on the MCU, humidity sensor and accelerometer. The MCU takes one reading from the humidity sensor and turns it off before the temperature sensor is turned on to avoid conflict between the sensors. One temperature reading is taken using the shared ADC pin before temperature sensor is turned off. After that, the MCU takes a total of three readings (one each from *x*-, *y*-, and *z*-axis) for each sampling from the accelerometer every 10 ms in the studied case, which can be suitable for sampling low vibration frequency of up to 50 Hz. Each reading is 2 bytes of data and is stored in the internal MCU RAM after each measurement. The MCU repeatedly takes reading from the accelerometer until a pre-defined number of readings are made, for example, a total of 48 readings for 16 times of sampling the accelerometer, which correspond to 96 bytes of data to ensure there are enough readings to cover the measured vibration frequencies in the studied case of this paper. Then, the MCU measures the storage capacitor voltage V_{CS} to judge whether V_{CS} is larger than V_{end} in the capacitor C_S for the MCU to take another 48 readings from the accelerometer and transmit all the data stored in the RAM. If so, the MCU will take another 48 readings from the accelerometer, store it in the RAM, and measures V_{CS} again. If not, the MCU transmits all the data stored in the RAM and sends a LOW signal to RESET pin of the voltage supervisor. The voltage supervisor then turns off the N-MOSFET so that the WSN goes into non-active phase and the cycle repeats, alternating between active phase and non-active phase as long as there is energy from the energy harvester. The data size to be transmitted in the first packet is 100 bytes, which consists of the readings from all three sensors and the remaining packets only have 96 bytes from the 48 accelerometer readings. For the implemented WSN program, it should be noted that there is only one transmission at the end of the active time just before the WSN is switched off for energy saving, for example, avoiding repeatedly setting up the transmission channel in the case of multiple transmissions.

D. *Determination of V_{end}*

The V_{end} can be determined by (1), which is based on the energy stored in the capacitor C_S and the energy required for the WSN to perform the next tasks of sampling another 48 readings from the accelerometer and transmitting all the data stored in the RAM.

$$\frac{1}{2}CV_{end}{}^2 - \frac{1}{2}CV_{min}{}^2 \geq E_{required} = E_{tx-2} + (N+1) \times E_{tx-48} + E_{samp-48} + E_{reset} \quad (1)$$

where $E_{required}$ is the energy required for the WSN to perform the required tasks in the next process, $E_{tx\text{-}2}$ and $E_{tx\text{-}48}$, $E_{samp\text{-}48}$, and E_{reset} is the energy required for the WSN to transmit 2 data of the temperature and the humidity measurements and 48 data of the accelerations from the RAM, sample 48 data from the accelerometer, and reset the hardware, respectively. N is the number of cycle of the WSN operations, and V_{min} is set to be 2.4 V, which is the minimum operating voltage of the MCU for the sensors operation without data losses. $E_{tx\text{-}2}$, $E_{tx\text{-}48}$, $E_{samp\text{-}48}$, E_{reset} can be determined through programming the WSN to perform the individual tasks and then measure the energy consumption of the tasks. For example, the WSN is programmed to only take 48 readings from the 3-axis accelerometer. One source meter

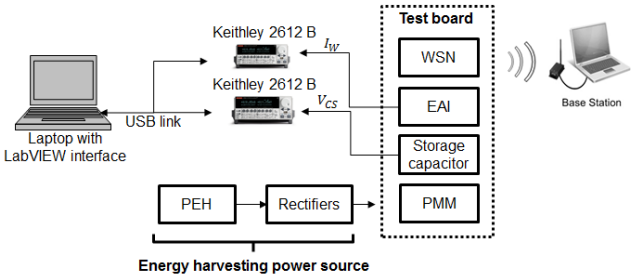

(a)

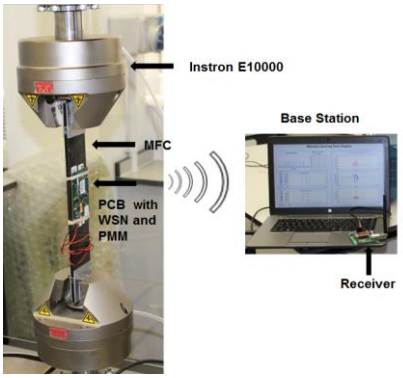

(b)

Fig. 5. (a) Block diagram of the experimental setup used for the characterization and (b) Images of the experimental setup for the PEH powered WSN to transmit data wirelessly to a base station.

(Keithley 2612B) can be used to measure the voltage V_s and current I_s supplied to the WSN, and then the energy consumption for performing the task can be calculated by (2).

$$E_{task}(t_n) = \sum_{k=1}^{n} V_s(t_k) I_s(t_k) \Delta t \tag{2}$$

where $E_{\text{task}}(t_n)$ is the energy consumption for the WSN to perform the individual tasks with the task time (t_n), $V_s(t_k)$ and $I_s(t_k)$ are the measured instantaneous voltage and current of the WSN at time t_k, Δt is the interval of the sampling time, and n is the sampling number during t_n. The subscript 'task' is the individual tasks of 'tx-2', 'tx-48', 'samp-48', or 'reset' depending on the program used to determine the energy consumption for the respective tasks. Using this method, $E_{\text{tx-2}}$, $E_{\text{tx-48}}$, $E_{\text{samp-48}}$, and E_{reset} has been found to be 8.75 µJ, 0.21 mJ, 3.34 mJ, and 0.17 mJ respectively in the studied case.

It should be highlighted that, on the second line of (1), it has been considered that energy E_{required} is guaranteed to be sufficient for transmitting all the data previously stored in the RAM when the case of $V_{CS} < V_{end}$ occurs immediately after the case of $V_{CS} > V_{end}$ if the capacitor size is properly chosen. This is because the energy calculation has included reserved energy (N+1 in the equation) for the transmission of data stored in the RAM which was obtained from the previous operation. Also, V_{end} is higher than V_{min} of the minimum operating voltage of the WSN, giving extra margin to the energy availability for performing the tasks. The proper capacitance C_S can be determined by the energy consumed by the required tasks. As the energy consumed by the WSN is known, determined by (2), a proper capacitance can be chosen to ensure successful operation of the WSN for all its required tasks. For example, at least 2 mF of capacitance is required to implement the first cycle of the measurement and transmission with 3.2 mW power generated by a PEH studied in the paper. If the capacitance were smaller than 2mF and as the WSN consumes almost fixed amount of energy for the required certain tasks in one cycle, V_{CS} would drop, possibly below V_{min}, which would make the WSN fail to complete its measurements, execute the energy-aware program and transmit the data. A proper capacitance, therefore, needs to be used for a number of cycle measurements so as to ensure there is enough energy for the WSN operation.

III. Experimental Methods

A. Experimental Setup

Experimental tests based on the custom developed energy harvesting powered WSN, shown in Fig. 1, were performed to understand the advantages of the energy-aware approaches. The experimental setup used is shown in Fig. 5, where two LabVIEW interfaces are used, one for real-time recording and displaying the transmitted sensor data to the base station placed at a distance of 4 m to verify the operation of the energy-aware approaches and one for real-time recording and displaying the measured voltage V_{CS} and current I_w to understand the advantages of the energy-aware approaches. Two Sourcemeters (Keithley 2612B) were used to measure the voltage V_{CS} and current I_w. A piezoelectric strain energy harvester using a macro-fiber composite (MFC) bonded on one side of a carbon fiber composite plate is used to scavenge ambient vibrational energy. An Instron E10000 ElectroPuls dynamic testing machine is used to apply strain vibration load to the energy harvester. The PCB with the WSN and the PMM is mounted on another side of carbon fiber composite plate. Although different sizes of capacitor has been tested, only 10 mF supercapacitor is used to show the results of the energy-aware approaches for the energy storage to power the energy-aware WSN in Section 4 of this paper as they give very similar results.

B. Configuration Characterization

To understand the advantages of the energy-aware approaches for the energy harvetsing powered WSN, characterizations and comparisons of 3 different configurations were performed. Configurations 1 and 2 are the developed energy harvesting powered WSN with the EAI shown in Fig. 1 and without the EAI by removing the EAI block in Fig.1 respectively, to study the EAI advantage in enabling the WSN operation without start-up problem when there is a limited energy harvested. Configuration 3 is the developed WSN powered by a DC power source without the EAI and is used to study the advantage introduced by the EAI for low sleep current consumption. In Configuration 3, a DC power source (Keithley 2220-30-1) is used to replace the MFC, EAI, and PMM to power the C_S and WSN and the MCU is programmed to run in a normal sleep mode, by using one wakeup timer clocked by its internal 32 kHz resistor-capacitor oscillator to generate a wake-up event. Following a wakeup event, the timer continues to run and the sleeping time is set by the wake-up timer. Moreover, to make fair comparisons between Configurations 1

and 3, the active and sleeping time of Configuration 3 is set to be the same as Configuration 1.

For the similar reason to the chosen capacitor size, for the testing of Configuration 1 and 2, in spite of different strain loadings which emulate aircraft wing strain loading have been applied onto the piezoelectric strain energy harvester through Instron E10000 testing machine, only the peak-to-peak strain loading of 600 με at 10 Hz with the 3.2 mW power generated by a piezoelectric energy harvester (PEH) was used to show the results in Section 4 of this paper. For Configuration 3 testing, the voltage of the DC power source is set to be 3.16 V, which is taken from the turn-on voltage for the energy-aware WSN in Configuration 1 to operate, and the input current is set to be 8 mA, which is the minimum current found by manually tuning that enables the operation of Configuration 3.

C. *Calculated average sleep current*

The average sleep current of the WSN presented in Section 4 is calculated based on:

$$I_{ave} = \frac{\sum_{k=1}^{n} I_w(t_k)\Delta t}{T_{sleep}} \quad (3)$$

where I_{ave} is the average sleep current of the WSN during the sleeping time T_{sleep}, I_w (t_k) is the instantaneous sleep current of the WSN at t_k, Δt is the interval of the sampling time and n is the total sampling number during T_{sleep}.

IV. Experimental Results and Discussions

A. *For Configuration 1*

The measured voltage of V_{CS} and current of I_w from Configuration 1 are shown in the Fig. 6. It shows that, from the beginning to 22.56 s, the capacitor was charged by the PEH and its voltage V_{CS} increased steadily from zero to 3.16 V. During this period, the voltage V_{CS} is below the pre-set threshold V_{on} of 3.16 V and so the WSN is off. As soon as V_{CS} reaches 3.16 V, the EAI turns on the N-MOSFET switch, enabling the capacitor to release its energy to the WSN. It also shows that, after initial charging of the capacitor for about 22.56 s, the PEH was able to power the WSN for a period of 1.15 s (active time) every 7.79 s (sleeping time) with a limited energy harvested of 3.2 mW by the PEH subject to a peak-to-peak strain loading of 600 με at 10 Hz vibration. Consequently, a drop in V_{CS} and a surge in I_w is observed in Fig. 6 (a) and (b) respectively as the WSN is switched into its active phase for about 1.15 s, including 0.17 s (wake up), 0.06 s (1 reading from the temperature and humidity sensors respectively), 0.64 s (the total sampling time of the accelerometer for 4 cycles), 0.12 s (the total judgement time for 4 cycles),0.14 s (transmission for 388 bytes of measured data) and 0.02 s (resetting WSN), shown in Fig. 6 (c).

During the active phase, the energy-aware program

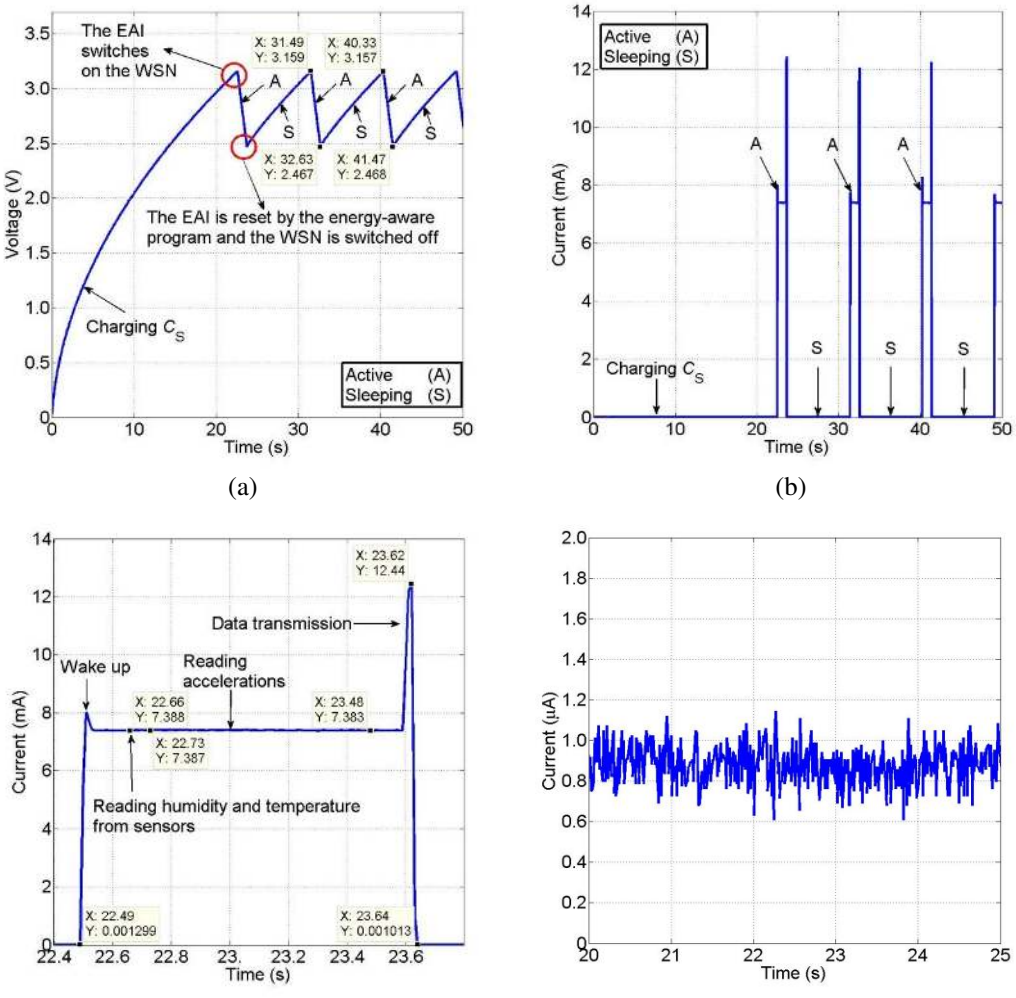

Fig. 6. Time dependence of (a) the voltage V_{CS}, (b) the current I_w with enlarged plots (c) during a complete active time and (d) during the sleeping time from Configuration 1.

calculates the V_{end} and resets the EAI once V_{CS} drops below the V_{end} of about 2.58 V, calculated from (1) and based on the V_{min} is set to be 2.4 V in the studied case. Therefore, the WSN was switched off at around 2.47 V of V_{off}, as shown in Fig. 6(a), which is slightly higher than 2.4 V. This shows that the V_{end} and V_{off} are not the V_{min}. As the given specific meaning of V_{end}, the implemented WSN will be able to have enough energy to complete all the measurement tasks and transmit all the data in the end of active time.

During the sleeping time, the WSN is turned off by the EAI, consuming an average current of 0.95 µA, calculated from the result shown in Fig. 6 (d) and based on (4). The main reason for the WSN to have such a low sleep current is that the EAI is able to switch off the WSN including the MCU and other sub-circuits during the sleeping time and so the power consumption of the WSN is almost zero. It can be analyzed that this average sleep current is mainly consumed by the voltage supervisor and N-MOSFET in the EAI.

B. *For Configuration 2*

The measured voltage of V_{CS} and current of I_w from Configuration 2 are shown in Fig. 7. It can be observed that V_{CS} was able to increase to 2.0 V and then fluctuated around it. When V_{CS} reaches the minimum turn-on voltage of the MCU (2.0 V), this voltage level can support some peripherals of the MCU such as the ADCs, DACs, comparators and the internal temperature sensor to start working, but it is lower than the minimum operating voltage of the MCU (2.4 V) to support all the peripherals of the MCU. However, those aforementioned parts are always powered on until there is a minimum operating voltage available to the core processor of the MCU for it to operate properly and control all the peripherals with proper initialization. Therefore, with the MCU continuously draws energy when the voltage supply is below the minimum operating voltage while there is a limited energy harvested by the PEH (3.2mW), the harvested energy cannot be accumulated in the energy storage.

It can also be observed that although the energy harvested by the PEH can support the WSN with up to 3 mA of current during the active time, the supplied current soon drops to around 0.313 mA, calculated from Fig. 7 (b). As the supplied current is much lower than the average current, required by the

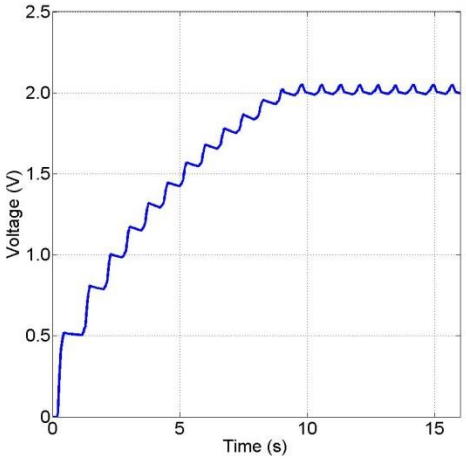

(a)

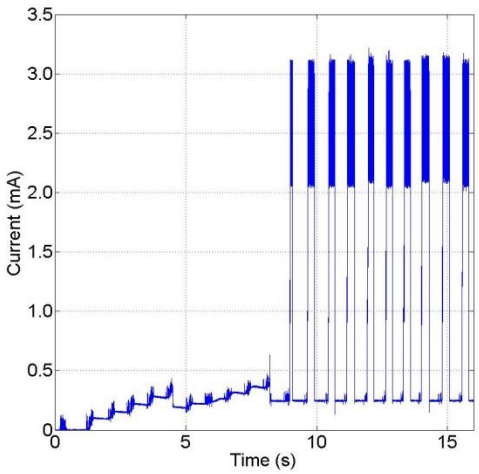

(b)

Fig. 7. Time dependence of (a) the voltage V_{CS}, and (b) the current I_w from Configuration 2.

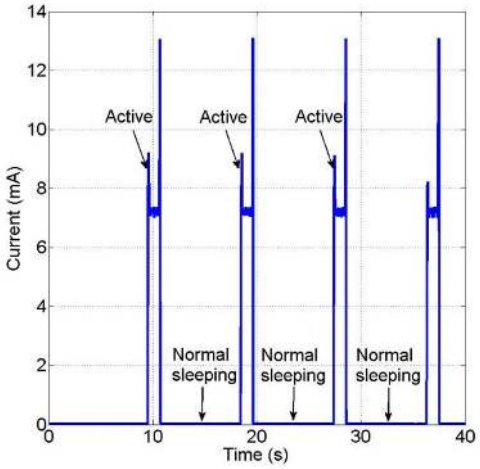

(a)

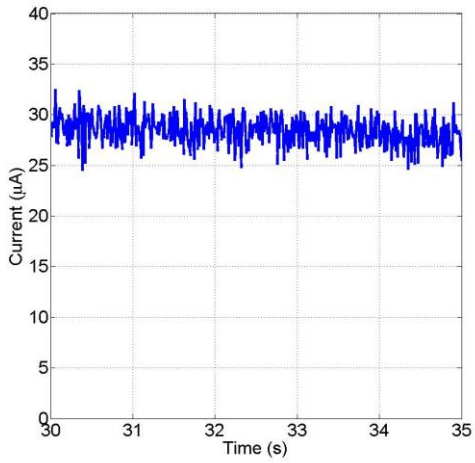

(b)

Fig. 8. Time dependence of the current I_w with the MCU running (a) in a normal sleep mode and (b) the detailed plot.

TABLE I
COMPARISONS OF THE PERFORMANCE AND AVERAGE NON-ACTIVE CURRENTS OF THE WSN WITH THE THREE CONFIGURATIONS

No	Configuration	Addition feature	Performance	Non-active phase current (μA)
1	PEH powered WSN with EAI	Energy-aware program	WSN able to work	0.95
2	PEH powered WSN without EAI	MCU running in a normal sleep mode	V_{CS} increases to about 2 V but WSN is not able to start	316
3	DC power Source powered WSN without the EAI	MCU running in a normal sleep mode	WSN is able to start and operate	28.3

WSN to start the operation, of around 8 mA, shown in Fig. 6(c), Configuration 2 without EAI is not able to start its operation. The similar reason as above is that the energy stored in the capacitor is immediately consumed by the WSN when the V_{CS} reaches the minimum turn-on voltage of the WSN. This means that the energy harvested could not be accumulated in the capacitor until it is enough for the operation of the WSN.

C. For Configuration 3

The measured voltage of V_{CS} and current of I_w from Configuration 3 are shown in Fig. 8. From Fig. 8(a), the active phase current consumption and pattern is similar to Configuration 1, as shown in Fig. 6(b), as the MCU was programmed to do similar tasks. However, from Fig. 8(b), it can be observed that the average sleep current of the system for Configuration 3 is around 28.3 μA. It can be analyzed that the current is mainly consumed by the internal wake-up timer, CPU processing, and 32 kHz crystal oscillator of MCU, which are used to control the MCU from sleep to wake up and also the associated sensor circuits.

D. Comparisons of the Three Configurations

The performances and the non-active phase currents of the three configurations are summarized in Table 1. Comparing configuration 1 and 2, it can be seen that the EAI plays an important role in dealing with the mismatch between the energy generated by the harvesters and the energy demanded by the WSNs to perform required tasks and in enabling the WSN to be powered by energy harvesting technology when there is a limited energy harvested. This is because the EAI enables the energy generated during the non-active phase to be accumulated in the capacitor without being immediately consumed by the WSN. Comparing configurations 1 with 3, it can be seen that the EAI can reduce the power consumption of the WSN during the sleeping time from 28.3 μA of a normal sleep mode to 0.95 μA since with the EAI, the internal wake-up timer and other associated circuits which consume more energy than the EAI are switched off.

V. CONCLUSION

This paper has reported a combined EAI with energy-aware program to manage the energy flow from the energy storage capacitor to the WSNs to deal with the mismatch between the energy generated by the harvesters and the energy demanded by the WSNs to carry out required tasks. These combined energy-aware approaches were implemented and experimentally studied in a custom developed piezoelectric vibration energy harvesting powered WSN. The experimental results show that, with a limited energy harvested, the combined energy-aware approaches enable (1) the harvested energy to be accumulated in the capacitor to deal with the mismatch for enabling the WSN operation, (2) solve the start-up issue, and (3) allow the WSN to have a low sleep current from 28.3 μA of a commercial WSN to 0.95 μA. It is also shown that the WSN without the combined energy-aware approaches is not able to start and therefore cannot operate when there is a limited energy harvested, which demonstrates the importance of the energy-aware approaches developed in this paper.

REFERENCES

[1] Y. Kuang, and M. Zhu, "Characterisation of a knee-joint energy harvester powering a wireless communication sensing node," *Smart Mater. Struct.,* vol. 25, no. 5, pp. 055013 (11 pp), 2016.

[2] S. Sudevalayam, and P. Kulkarni, "Energy harvesting sensor nodes: Survey and implications," *IEEE Commun. Surv. Tut.,* vol. 13, no. 3, pp. 443-461, 2011.

[3] D. Guyomar, and M. Lallart, "Recent progress in piezoelectric conversion and energy harvesting using nonlinear electronic interfaces and issues in small scale implementation," *Micromachines,* vol. 2, no. 2, pp. 274-294, 2011.

[4] A. D. T. Elliott, and P. D. Mitcheson, "Implementation of a single supply pre-biasing circuit for piezoelectric energy harvesters," *Procedia Eng.,* vol. 47, pp. 1311-1314, 2012.

[5] T. C. Huang, M. J. Du, Y. C. Kang, R. H. Peng, K. H. Chen, Y. H. Lin, T. Y. Tsai, C. C. Lee, L. D. Chen, and J. L. Chen, "120 % harvesting energy improvement by maximum power extracting control for high sustainability magnetic power monitoring and harvesting system," *IEEE Trans. Power Electron.,* vol. 30, no. 4, pp. 2262-2274, 2015.

[6] J. Zhang, P. Li, Y. Wen, F. Zhang, and C. Yang, "A management circuit with upconversion oscillation technology for electric-field energy harvesting," *IEEE Trans. Power Electron.,* vol. 31, no. 8, pp. 5515-5523, 2016.

[7] C. Alippi, and C. Galperti, "An adaptive system for optimal solar energy harvesting in wireless sensor network nodes," *IEEE Trans. Circuits Syst. I, Reg. Papers,* vol. 55, no. 6, pp. 1742-1750, 2008.

[8] W. Wang, V. Cionca, N. Wang, M. Hayes, B. O'Flynn, and C. O'Mathuna, "Thermoelectric energy harvesting for building energy management wireless sensor networks," *Int. J. Distrib. Sens.Netw.,* vol. 2013, pp. 14, 2013.

[9] N. Kong, and D.-S. Ha, "Low-power design of a self-powered piezoelectric energy harvesting system with maximum power point tracking," *IEEE Trans. Power Electron.,* vol. 27, no. 5, pp. 2298-2308, 2012.

[10] Y. K. Tan, and S. K. Panda, "Optimized wind energy harvesting system using resistance emulator and active rectifier for wireless sensor nodes," *IEEE Trans. Power Electron.,* vol. 26, no. 1, pp. 38-50, 2011.

[11] F. Entezami, M. Zhu, and C. Politis, "How much energy needs for running energy harvesting powered wireless sensor node?," *Energy Harvesting Syst.,* vol. 3, no. 3, pp. 197-203, 2016.

[12] R. Torah, P. Glynne-Jones, M. Tudor, T. O. Donnell, S. Roy, and S. Beeby, "Self-powered autonomous wireless sensor node using vibration energy harvesting," *Meas. Sci. Technol.,* vol. 19, no. 12, pp. 125202 (8 pp), 2008.

[13] Texas Instruments Incorporated, "Mixed signal microcontroller datasheet," Rep. no. MSP430F22x2, MSP430F22x4, Datasheet., 2012. [Online]. Available: http://www.ti.com/lit/ds/slas504g/slas504g.pdf. Accessed on Jan. 04, 2017.
[14] NXP Laboratories UK, "JenNet, ZigBee PRO and IEEE802.15.4 module," Rep. no. JN5148-001-Myy, Datasheet., 2010. [Online]. Available: http://www.glynstore.com/content/docs/jennic/JN-DS-JN5148MO-1v4.pdf. Accessed on Jan. 04, 2017.
[15] M. Minami, T. Morito, H. Morikawa, and T. Aoyama, "Solar biscuit: A battery-less wireless sensor network system for environmental monitoring applications," in *The 2nd Int. Workshop on Netw. Sens. Syst.*, San Diego, California USA, 2005.
[16] V. Marsic, M. Zhu, and S. Williams, "Wireless sensor communication system with low power consumption for integration with energy harvesting technology," *Telfor J.,* vol. 4, no. 2, pp. 89-94, 2012.
[17] M. Ferrari, F. Cerini, and V. Ferrari, "Autonomous sensor module powered by impact-enhanced energy harvester from broadband low-frequency vibrations," *Transducers & Eurosensors XXVII.* pp. 2249-2252.
[18] R.-G. Lee, K.-C. Chen, C.-C. Lai, S.-S. Chiang, H.-S. Liu, and M.-S. Wei, "A backup routing with wireless sensor network for bridge monitoring system," *Measurement,* vol. 40, no. 1, pp. 55-63, 2007.

Tingwen Ruan received his BEng degree in 2012 from the Nanjing University of Posts and Telecommunications, China. He joined the Energy Harvesting Research Group at the University of Exeter in the UK, in 2014 as a PhD student. Prior to starting his PhD study, he worked as a technical support engineer in the Zhongxing Telecommunication Equipment Corporation, China (2013).
His current research interest is in the area of energy harvesting powered wireless sensing nodes and networks for structural health and environmental monitoring.

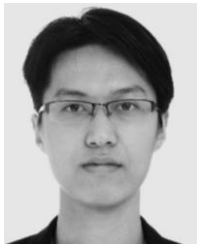

Zheng Jun Chew received his BEng degree in 2010 from the University of Strathclyde, Glasgow and PhD degree in 2014 at Swansea University, UK. He joined the Energy Harvesting Research Group at the University of Exeter in the UK, in 2014 as an Associate Research Fellow. Prior to pursuing his PhD, he worked as an electrical engineer in Sony EMCS (M) Sdn. Bhd., Malaysia (2010).
His current research interest is in the area of power management module for piezoelectric energy-harvesting devices. He has published more than 10 refereed journal papers and one book chapter.

Meiling Zhu received her BEng degree in 1989, MEng in 1992, and PhD in 1995 at Southeast University, Nanjing, China. She currently holds the Professor and the Chair in Mechanical Engineering and the Head of Energy Harvesting Research Group in the University of Exeter in the UK. Prior to joining the University of Exeter, She worked in a number of Universities: Cranfield University (2002-13), the University of Leeds (2001-2); Stuttgart Universität (1999-2001); the Hong Kong University of Science and Technology (1998-9); and the Institute of Vibration Engineering Research, in the Nanjing University of Aeronautics & Astronautics (1994-98).
Her current research interests are in the area of piezoelectric energy harvesting powered wireless sensor nodes for applications.